CHAPTER

Cellular and subcellular context determine outputs from signaling biosensors

15

Dominic Devost*, Nicolas Audet*, Cynthia Zhou*, Hiroyuki Kobayashi§, Hélène Bonin§, Viktorya Lukashova§, Christian Le Gouill§, Michel Bouvier§, Terence E. Hébert*,1

**Department of Pharmacology and Therapeutics, McGill University, Montréal, QC, Canada*

§Department of Biochemistry and Molecular Medicine, Institute for Research in Immunology and Cancer, Université de Montréal, Montreal, QC, Canada

[1]Corresponding author: E-mail: terence.hebert@mcgill.ca

CHAPTER OUTLINE

Introduction and Rationale 320
Introduction 320
Rationale and Objectives 321
1. Materials and Instrumentation Required 322
1.1 Reagents 322
1.2 Biosensor and Receptor Plasmid Construction 323
1.2.1 Receptor expressing plasmids 323
1.3 Instrumentation 323
2. Basic Methodology 323
2.1 Tissue Culture and Transfection 323
2.2 BRET Measurements 325
3. Experimental Strategies 326
3.1 Sensor Design 326
3.2 Sensor Validation 326
3.3 Nuclear ERK Activation Measured Using the BRET-Based ERK-NLS Sensor in Different Heterologous cell models 328
3.3.1 Theory 328
3.3.2 Experimental workflow 328
3.3.3 Results 328
3.4 Nuclear ERK Activation Measurements Using the BRET-Based ERK-NLS Sensor in an Endogenous Cell Model 330
3.4.1 Theory 330

Methods in Cell Biology, Volume 132, ISSN 0091-679X, http://dx.doi.org/10.1016/bs.mcb.2015.11.010

3.4.2 Experimental workflow 332
3.4.3 Results 332
4. Discussion **335**
Acknowledgments **335**
References **336**

Abstract

The use of biosensors either individually or as part of panels has now become a common technique to capturing signaling events in living cells. Such biosensors have become particularly important for probing biased signaling and allostery in G protein-coupled receptor drug screening efforts. However, assumptions about the portability of such biosensors between cell types may lead to misinterpretation of drug effects on specific signaling pathways in a given cellular context. Further, the output of a particular biosensor may be different depending on where it is localized in a cell. Here, we discuss strategies to mitigate these concerns which should feed into future biosensor design and usage.

INTRODUCTION AND RATIONALE

INTRODUCTION

The use of biosensors to track cellular signaling events in live cells and tissues is transforming our ability to measure multiple signaling pathways in a manner compatible with high throughput and high content screening (Domazet et al., 2015; Namkung et al., 2015; Sauliere et al., 2012). The advantages of such approaches are obvious as they allow monitoring of diverse cell responses evoked by compounds with reliable spatio-temporal resolution. As compound libraries increase in size and robotics and automation make screening such libraries possible, adaptation of signaling assays to homogenous cell-based platforms enables such screens. Further, the idea that receptors such as G protein-coupled receptors (GPCRs) are wired into multiple signaling pathways in a given cell makes parallel measurements of multiple pathways using such biosensors a way to generate large sets of pertinent data from individual screens. Finally, it has become clear that many ligands selectively regulate subsets of the entire receptor signalosome, a notion known as biased agonism or functional selectivity. Screening larger sections of the signalosome allows stratification of ligands according to such bias, facilitating the identification of drugs with better side effect profiles and increased therapeutic benefit (Kenakin & Christopoulos, 2013a, 2013b; Luttrell, 2014). Building panels of biosensors is relatively easy and there was hope that such sensors would generate robust responses in whatever cells they are placed in. However, as we demonstrate below, this cannot be taken for granted even in cells where the same GPCR is transfected and the same signaling pathway operates. Further, we also discuss considerations about biosensors that are localized to distinct subcellular sites within the same

cell. For the purpose of this discussion, we focus on a biosensor designed to capture ERK1/2 signaling events in the nucleus.

The MAPK (mitogen-activated protein kinase) family is comprised of a class of serine/threonine protein kinases that include the extracellular signal-regulated kinase 1 and 2 (ERK1/2), ERK5, p38, and the cJun N-terminal kinase (JNK). ERK1/2 is essential for a wide range of cellular functions including differentiation, proliferation, and survival of many different cell types. ERK activity is dysregulated in many cancers (Thomas & Huganir, 2004), plays an important role in tumorigenesis, and is also associated with multiple neurological disorders (Kim & Choi, 2010).

The best-studied signaling cascade that engages ERK1/2 is the Ras-Raf-MEK-ERK pathway, where Ras (Ras-GTP) binds Raf-1 directly and recruits it to the membrane. Raf subsequently becomes activated, phosphorylates and activates MEK1 and MEK2 (the MAPK kinase), which in turn binds and phosphorylates ERK1 and ERK2 (Chang & Karin, 2001). Activation of numerous receptor systems has been shown to modulate the ERK1/2 cascade via different inputs into the Ras-RAF-MEK-ERK cascade. These include receptor tyrosine kinases, integrins, ion channels, and different families of GPCRs. For GPCRs, both G protein- or β-arrestin-dependent pathways have been shown to activate MAPK (Tohgo, Pierce, Choy, Lefkowitz, & Luttrell, 2002; Wei et al., 2003). In cells, ERK1/2 signaling is often localized to the cytoplasm. However, activated ERKs also translocate to the nucleus and directly phosphorylate transcriptional regulatory proteins. Methods to detect activation of ERK1/2 at specific cellular sites would offer useful tools to probe activity in different subcellular compartments such as the nucleus.

RATIONALE AND OBJECTIVES

To monitor MAP kinase activity, a variety of biochemical techniques including Western blotting, immunocytochemistry, and ELISA are routinely used. These assays generally rely on the use of antibodies raised against the active form of ERK1/2 and therefore limit detection of ERK activity to fixed tissues, permeabilized cells, or lysate preparations. To monitor MAP kinase pathway activation in intact cells and in real time at specific subcellular sites, genetically encoded biosensors have been developed using resonance energy transfer (RET). A FRET-based sensor called EKAR (extracellular-regulated kinase activity reporter) sensor has been used to track ERK1/2 activity (Harvey et al., 2008). FRET is a nonradiative energy transfer between a compatible pair of fluorophores that, in this case, is CFP (donor) and YFP (acceptor). Energy transfer depends on (1) the overlap between the emission spectra of the donor and excitation spectra of the acceptor, (2) the relative orientation of donor and acceptor, and (3) their relative distance; FRET occurs when the donor and the acceptor are separated by less then 100 Å. The CFP and YFP moieties of the EKAR sensor are separated by a specific peptide substrate of ERK1/2 and a domain recognizing and binding this peptide substrate when phosphorylated by ERK1/2. Binding of the phosphosensor to the ERK-phosphorylated peptide sequence

promotes a conformational change in the biosensor that brings the energy donor and acceptor into closer proximity thus yielding an increased FRET signal. Because FRET-based sensors require incident excitation by strong light sources that can result in autofluorescence and direct activation of the acceptor, they are less suitable for high-throughput screening in a plate format. To avoid these limitations, we designed a novel BRET (bioluminescence RET)-based biosensor detecting ERK1/2 phosphorylation events. BRET uses the same energy transfer principle as FRET except that the energy donor is a bioluminescence enzyme, often *Renilla* luciferase (Rluc, Galés et al., 2005). Using this approach, an external light source is not required, avoiding the necessity for spectral corrections required in FRET experiments and facilitating detection of small RET signals. This novel biosensor uses ERK1/2 phosphorylation sites from Cdc25C, WW phospho-acceptor domains from Pin1 and an ERK1/2 docking site from $P90^{RSK}$. The addition of a nuclear localization sequence (NLS) allows assessment of nuclear ERK1/2 activation by different receptor agonists, PKC or EGF in different cellular contexts. In this chapter, we describe the design of the biosensor, how it was expressed, how it behaved in different cell lines, and how biosensor activity was assessed using BRET.

1. MATERIALS AND INSTRUMENTATION REQUIRED

1.1 REAGENTS

Where reagents are unique or difficult to obtain, we provide a source.
HEK 293 cells
HeLa cells
AC16 cells (obtained from Dr Mercy Davidson, Columbia University)
D-MEM
DMEM/F12
L-Glutamine
trypsin-EDTA solution
MEM
FBS
Penicillin and streptomycin
Kreb's/HEPES (146 mM NaCl, 4.2 mM KCl, 0.5 mM $MgCl_2$, 1 mM $CaCl_2$, 5.9 mM glucose, 10 mM HEPES, pH 7.4).
Lipofectamine 2000 (Invitrogen)
Polyethylenimine 25 kDa, linear (PEI)
Tyrode's solution (140 mM NaCl, 2.7 mM KCl, 1 mM $CaCl_2$, 12 mM $NaHCO_3$, 5.6 mM D-glucose, 0.49 mM $MgCl_2$, 0.37 mM NaH_2PO_4, and 25 mM HEPES at pH 7.4)
Polyornithine
Phosphate buffer solution (137 mM NaCl, 2.7 mM KCl, 10 mM Na_2PO_4, and 0.2 mM KH_2PO_4, at pH 7.4)

Gelatin
Flat bottom white 96-well plate (Costar)
Ethanol (90% pure)
DMSO
Coelenterazine 400a (Goldbio, St. Louis, MO, USA)
Phorbol 12-myristate 13-acetate (PMA, Sigma)
Epidermal growth factor (EGF, Fitzgerald, Acton, MA, USA)
Carbamylcholine chloride (Carbachol, Sigma)
Arginine vasopressin (AVP, Sigma)
Angiotensin II (Ang II, Sigma)

1.2 BIOSENSOR AND RECEPTOR PLASMID CONSTRUCTION

ERK biosensor: The ERK-NLS biosensor expressed in a pIRESB plasmid is illustrated in Figure 1(A). It contains RLucII (Leduc et al., 2009) at its N-terminus, two WW domains from Pin1 (amino acids 1−54 of human Pin1 (Sudol & Hunter, 2000)), a linker of 300 amino acids forming a disorganized and flexible structure, four phospho-acceptor sites from Cdc25C (Busino, Chiesa, Draetta, & Donzeli, 2004), GFP10, an ERK docking site (D-domain, Ddom) from $P90^{RSK}$ ((Dimitri, Dowdle, MacKeigan, Blenis, & Murphy, 2005), PIESSILAQRRVRKLPSTTL), and a NLS from the SV40 Large T-antigen (PKKRKVEDA) at the distal C-terminus.

1.2.1 Receptor expressing plasmids

Plasmid vectors encoding different GPCRs: N-terminally FLAG-tagged M3 muscarinic acetylcholine receptor (M3R) inserted into pcDNA3 (a generous gift from Dr Jean-Luc Parent, Université de Sherbrooke), and N-terminally tagged Myc V2 vasopressin receptor (V2R) inserted into pRK5 (a generous gift from Dr Marc Thibonnier, Case Western Reserve University).

1.3 INSTRUMENTATION

The sensors we have used can be measured in any modern, RET-enabled plate reader. We used a Fluostar Optima plate reader from BMG with luminescence detection capability and a BRET2 filter set (410/80 and 515/30 nm) that allows sequential integration of light signals detected with two filter settings. For increased sensitivity, we also used a Victor X-Light plate reader from Perkin−Elmer with luminescence detection capability and a BRET2 filter set (410/80 and 515/30 nm).

2. BASIC METHODOLOGY

2.1 TISSUE CULTURE AND TRANSFECTION

HEK 293 and HeLa cells were respectively cultured in DMEM supplemented with 5% FBS and MEM supplemented with 10% FBS, penicillin, and streptomycin at

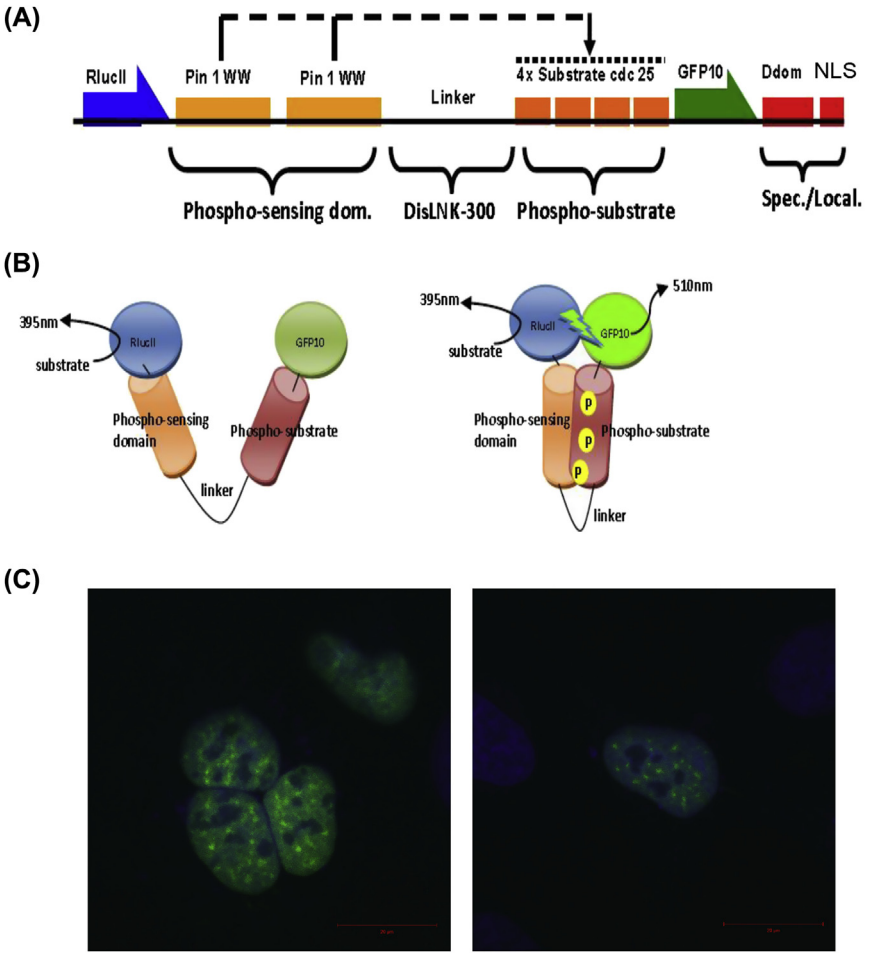

FIGURE 1 BRET (bioluminescence resonance energy transfer)-based extracellular signal-regulated kinase—nuclear localization sequence (ERK-NLS) sensor structure and cellular localization.

(A) The design of the ERK-NLS sensor. It contains an N-terminal *Renilla* luciferase II (RlucII), two WW domains from Pin1, a flexible 300 amino acid linker, four phospho-acceptor sites from Cdc25C, GFP10, an ERK docking site (Ddom) from $P90^{RSK}$, and an NLS from the SV40 large T-antigen. (B) Illustration of the detection mode for ERK-mediated phosphorylation of the biosensor in the inactive state (left panel) or following activation of ERK1/2 (right panel). (C) Nuclear localization of the ERK-NLS sensor transiently expressed in HEK 293 cells detected by GFP fluorescence excited with 488 nm argon laser line and showing emission in 505–530 nm. Nuclei were stained with a blue (black in print versions) fluorescent DNA dye (DAPI) excited with 405 nm diode and emission in 420–480 nm. Images of nuclei were taken using a Zeiss LSM500 confocal microscope with 63x/1.04 Plan-Apochromat objective.

37 °C in a 5% CO_2 atmosphere. The day before transfection, cells were detached using a trypsin−EDTA solution and replated in the same culture media in 6-well plates and cultured for 24 h under the same conditions. The media was then aspirated and replaced with antibiotic-free media and cells were transfected with the ERK-NLS sensor in the presence or the absence of cDNA constructs for different GPCRs. Transfections were performed using Lipofectamine 2000 (Invitrogen) according to the manufacturer's recommendations. Twenty-four hours later, cells were replated in complete culture media onto polyornithine-coated white 96-well plates and BRET was assessed after another 24 h in culture.

AC16 cells (Davidson et al., 2005) were cultured in DMEM/F12 supplemented with 10% FBS, 2 mM L-glutamine, penicillin, and streptomycin at 37 °C in 5% CO_2 atmosphere. Transfections were performed using PEI by reverse transfection. Briefly, 100 ng of plasmid DNA in 5 μL sterile PBS (per well) was mixed with 300 ng of PEI in 5 μL sterile PBS (per well) and incubated for 20 min. 10 μL of the DNA-PEI mix was added to each well of a 0.1% gelatin coated (1 h incubation followed by sterile PBS wash) white 96-well plate. Cells were detached using trypsin−EDTA solution and plated in DNA-PEI mix with DMEM/F12 supplemented with 5% FBS (10,000 cells; 100 μL per well). 16 h later, media was changed for complete culture medium. BRET was assessed 48 h posttransfection.

2.2 BRET MEASUREMENTS

BRET was recorded with plate readers that allow sequential integration of light signals detected with two filter settings and the BRET2 (BRET400-GFP) signal was calculated as the ratio between GFP10 emission at 515 nm and the light emitted by RlucII at 410 nm. All experiments were performed at 37 °C. Changes in BRET2 induced by the ligands/agonists were expressed as a "ΔBRET2 ratio" using the formula:

$$\Delta\text{BRET2 ratio} = \frac{\text{emission GFP}^{10}_{\text{ligand}}}{\text{emission Rluc}_{\text{ligand}}} - \frac{\text{emission GFP}^{10}_{\text{buffer}}}{\text{emission Rluc}_{\text{buffer}}}$$

The day of the experiment, HEK 293 or HeLa cells, cells were rinsed twice with Krebs buffer and maintained in the Krebs buffer (37 °C; 5% CO_2) for 3 h. BRET2 between RlucII and GFP10 was measured 3−5 min after the addition of the RlucII substrate coelenterazine 400a (5 μM final concentration), using a Fluostar Optima plate reader from BMG (see Section 1.2). Unless otherwise specified, all measurements were done in triplicate.

For AC16, cells were washed twice with Tyrode's solution and maintained in Tyrode's solution (37 °C; 5% CO_2) for 3 h. Concentration-response curves were generated by adding different concentrations of ligand at the same time as coelenterazine 400a (5 μM final). BRET2 between RlucII and GFP10 was measured every 5 min for 30 min after the addition of the ligand, using a Victor X-Light plate reader from Perkin Elmer (see Section 1.2).

For HEK 293 and HeLa cell experiments, kinetic studies were performed using a saturating concentration of the agonist and BRET was assessed at different times. Concentration-response curves were obtained by measuring BRET at different concentrations of the agonist at a fixed time that corresponded to the maximal response determined by kinetic studies. For experiments in AC16 cells, Emax was calculated by subtraction of the vehicle condition from the mean of the two highest concentrations of ligand where a plateau was reached. Kinetics were measured at Emax by sampling every 5 min. Statistical analysis was performed on Emax measured at 10 min (sufficient time for a plateau to be reached) using a paired Student's *t* test on BRET values comparing treated versus vehicle groups. Curve fitting was performed using Graphpad PRISM version 5.03.

3. EXPERIMENTAL STRATEGIES

3.1 SENSOR DESIGN

The ERK-NLS sensor is a unimolecular BRET-based MAP kinase activity detecting protein. As shown in the Figure 1(A), it is composed of multiple copies of a specific MAP kinase substrate and a phosphosensor domain linked together by a 300-amino-acid-long disorganized linker and flanked at the N-terminus by the BRET donor RlucII and at the C-terminus by the acceptor GFP10. To allow docking of activated ERK1/2 to the sensor and for localization to the nucleus, amino acid sequences coding for a D-domain and a nuclear localization signal were added respectively to the end of the protein. In the basal, nonactivated state, both donor and acceptor moieties are relatively distant from one another resulting in a low BRET signal as depicted in Figure 1(B) (left panel). Upon ERK-mediated phosphorylation of the substrate domain, binding of the phospho-sensing domain to the phosphorylated substrate domain stabilizes sensor folding bringing the BRET partners into closer proximity resulting in an increased BRET signal (see Figure 1(B), right panel).

3.2 SENSOR VALIDATION

Cellular localization of the sensor detected by immunofluorescence showed a strictly nuclear expression of ERK-NLS protein (see Figure 1(C)). Stimulation of HEK 293 cells transfected with the V2 vasopressin receptor with increasing concentrations of AVP resulted in a dose-dependent activation of ERK1/2 as reflected by biosensor activity which was essentially absent when the receptor was not transfected (Figure 2(A)). Stimulation with 10 ng/mL EGF in the presence of different pathway blockers showed that increased BRET from the ERK-NLS sensor could be repressed in a dose-dependent manner by two independent MEK inhibitors (U0126 and PD98059) as well as with a blocker of the EGF receptor (AG1478, Figure 2(B)). These experiments validated that the sensor captures activation of ERK1/2 and accurately reflects the involvement of MEK and activation via the

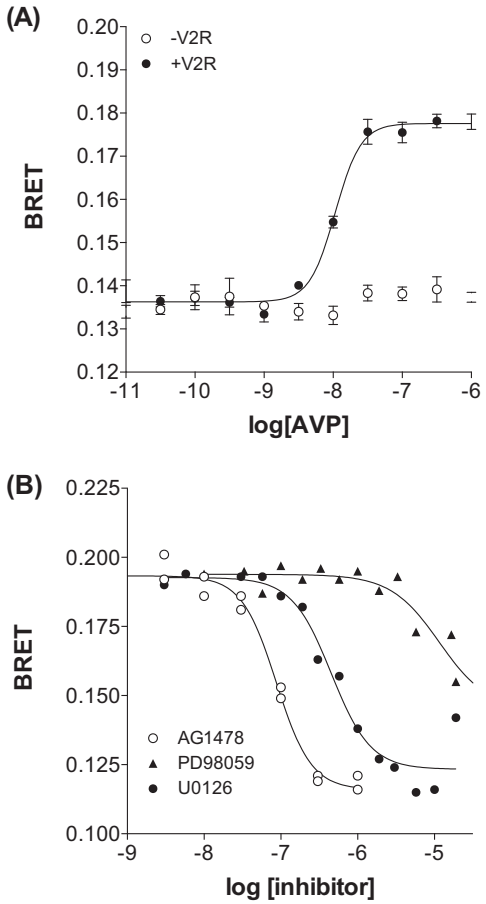

FIGURE 2 Arginine vasopressin (AVP)-induced sensor responses in HEK 293 cells.

(A) Dose-response curves for AVP stimulation in cells transiently expressing the ERK-NLS biosensor in presence or absence of co-transfected V2 vasopressin receptors. Cells were stimulated with increasing concentrations of AVP for 10 min followed by bioluminescence resonance energy transfer 2 (BRET2) measurements. Data are mean of ΔBRET $\pm$ SEM, n = 3. (B) Dose-response curves for stimulation by 10 ng/mL EGF for 10 min followed by BRET2 measurements with increasing concentrations of AG1478 (IC_{50} = 88 nM), PD98059, IC_{50} = 12 μM) or U1026 (IC_{50} = 450 nM). Data are mean of ΔBRET $\pm$ SEM, n = 3.

EGFR. Our BRET-based nuclear ERK1/2 biosensor is HTS-compatible for drug screening as Z′ determination from HEK 293 cells expressing the sensor showed values of $\sim$0.7 for both EGF- and PMA-induced (see below) ERK1/2 activation (data not shown).

3.3 NUCLEAR ERK ACTIVATION MEASURED USING THE BRET-BASED ERK-NLS SENSOR IN DIFFERENT HETEROLOGOUS CELL MODELS

3.3.1 Theory

As described above, our biosensor was designed to monitor nuclear ERK1/2 activity in real time in intact cells. In this section, we will detail the experimental workflow to monitor MAP kinase activation following stimulation by different upstream ERK1/2 activators including EGF, PMA, and different GPCRs in HEK 293 and HeLa cells, two commonly used cell lines for heterologous expression.

3.3.2 Experimental workflow

1. HEK 293 and HeLa cells were plated in six-well plates and transfected as described in Section 2.1.
2. 24 h posttransfection, 9000 cells were replated into wells of white flat bottom 96-well plates and maintained in complete media for an additional 24 h before the experiments These plates were pretreated with a sterile solution of 100 μg/mL polyornithine for 15−30 min at room temperature, washed with sterile water, and left to dry before use. On the day of the experiment, cells were washed with Kreb's buffer and maintained in 80 μL of the same buffer at 37 °C for 2−3 h to allow cell stabilization.
3. 10 μL of 50 μM coelenterazine 400A was then added and the plate left for 3 min at 37 °C.
4. BRET was assessed as described in Section 2.2 using the Fluostar plate reader. To measure the effect of drugs, 10 μL of a 10X concentrated solution containing the agonist was added to the well 3 min after coelenterazine addition and the plate was immediately put back into the plate reader. Luminescence and fluorescence were measured at 410/80 and 515/30 nm, respectively, at different times following ligand addition. Vehicle was added to other wells and BRET recorded the same way and subtracted from agonist-induced BRET to obtain drug-promoted BRET changes presented as ΔBRET (see Section 2.2).

3.3.3 Results

HEK 293 and HeLa cells were exposed to a saturating level of PMA, a direct activator of PKC that promotes PKC-mediated activation of ERK1/2, and BRET was assessed at different times. In both cell lines, an increase in BRET ratios was observed over time, albeit at different rates, that reached a maximum at 10 and 20 min post stimulation in HeLa and HEK 393 cells, respectively (Figure 3(A)). When monitoring nuclear ERK1/2 activity at different PMA doses, similar potencies for the PKC activator were measured in both cell lines (Figure 3(B)). These results again suggest that the sensor was functional in both cell lines and faithfully recorded activation of ERK1/2.

To test whether the sensor could detect nuclear MAP kinase activity in response to other GPCR agonists, we next stimulated HEK 293 cells with the muscarinic receptor agonist carbachol, acting on endogenous muscarinic M1 and M3 receptors

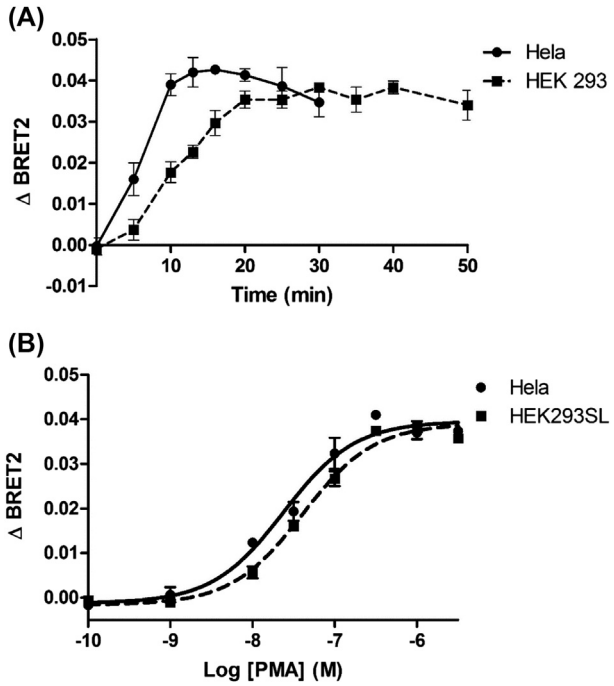

FIGURE 3 Effect of direct PKC activation by PMA on sensor activity in HEK 293 and HeLa cells.

(A) Kinetics of PMA stimulation. Bioluminescence resonance energy transfer 2 (BRET2) measurements were taken at intervals for the indicated period of time in presence of PMA (0.32 μM). Experiments were performed at 37 °C. Data are mean ± sd of triplicate wells. (B) Dose-response curves for PMA stimulation. Cells were stimulated with increasing concentrations of PMA for 16 min for HeLa or 30 min for HEK 293, respectively, followed by BRET2 measurements. Data are mean ± sd of triplicate wells.

(Khan et al., 2015) as well as cells transfected with a FLAG-tagged muscarinic M3 receptor. BRET responses were subsequently measured over time. We previously reported that activation of the endogenous muscarinic M3 receptor with carbachol leads to a transient but robust increase in ERK1/2 phosphorylation as detected by Western blotting (Khan et al., 2015). Surprisingly, no significant BRET from the sensor was detected over a similar period of observation (see Figure 4). Further, no carbachol effect was observed in cells in which the muscarinic M3 receptor was transiently overexpressed, under conditions where PMA (Figure 4) and EGF (data not shown) robustly induced a rapid sensor response.

This apparent lack of muscarinic M3 receptor-driven sensor responses in HEK 293 cells was surprising because, as previously mentioned, ERK1/2 activation could be detected upon carbachol stimulation in these cells by Western blot (Khan et al., 2015). This suggested that perhaps the localization of the sensor to the nucleus

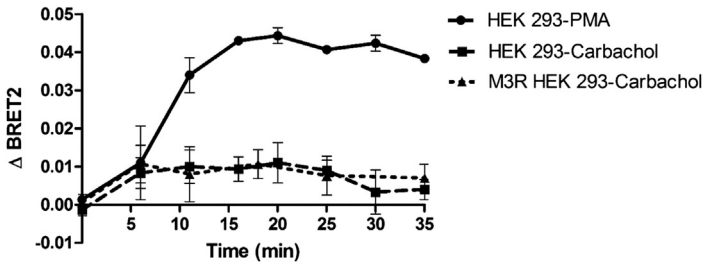

FIGURE 4 Comparison of PMA and carbachol sensor responses in HEK 293 cells.

Kinetic measurements were taken at intervals for the indicated period of time in presence of PMA (0.65 μM) or carbachol (1 mM). Response to carbachol was obtained in both the presence and absence of M3R overexpression. Experiments were performed at 37 °C. Data are mean ± sd of triplicate wells.

precluded it from recording general responses to the M3 receptor or that such responses were localized to the cytosol or other extranuclear compartments. To validate these observations in another heterologous cell line expressing endogenously the M3 receptor, similar experiments were conducted in HeLa cells (Deng, Sun, & Fang, 2013). As in HEK 293 cells, carbachol activation of endogenous M3 receptors did not trigger BRET changes in HeLa cells (data not shown). However, heterologous expression of M3 receptors led a dramatic increase in the carbachol response that peaked at 10 min and then gradually decreased (Figure 5(A)). In this condition, carbachol is therefore a highly potent receptor agonist for nuclear ERK1/2 activation (Figure 5(B)) as assessed by the NLS-ERK BRET-based biosensor. Similar observations were obtained when the V2 vasopressin receptor, was heterologously expressed (Figure 5(C) and (D)). Taken together, these data show that the sensor cannot readily detect nuclear ERK activity activated from low levels of endogenously expressed GPCR but generated a robust and reproducible BRET signal in the context of receptor overexpression, at least in heterologous cell models. Thus when generating and using biosensors, nontransfected receptor controls should always be performed as they may provide information about how the endogenous receptors may be wired distinctly from overexpressed receptors or may reflect the sensitivity of the assays. The level of activation promoted by the endogenous receptor may be too small to be detected thus increasing receptor levels would increase the signal detected. Our data also indicate that the same receptor expressed in different cell types may not activate ERK1/2 in the same compartments.

3.4 NUCLEAR ERK ACTIVATION MEASUREMENTS USING THE BRET-BASED ERK-NLS SENSOR IN AN ENDOGENOUS CELL MODEL

3.4.1 Theory

In this section, we will detail the experimental workflow to monitor ERK1/2 activation by stimulation of endogenous GPCRs in the cardiomyocyte model AC16

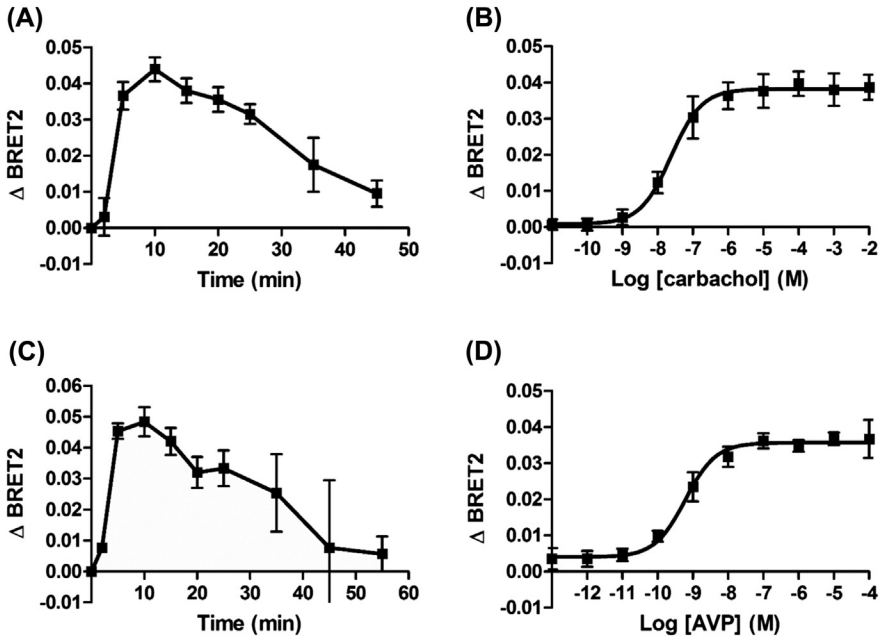

FIGURE 5 Carbachol-induced bioluminescence resonance energy transfer (BRET) changes in HeLa cells.

(A) Kinetic measurements were obtained in HeLa cells transiently expressing ERK-NLS biosensor in presence of co-transfected M3 muscarinic receptors. Values are means of ΔBRET done in triplicate ± sd. (B) Dose-response curves for carbachol stimulation. HeLa cells transiently expressing both the sensor and the M3 receptor were stimulated with increasing concentrations of carbachol for 10 min followed by BRET2 measurements. Data are mean of ΔBRET ± SEM, n = 3. (C) Kinetic measurements were made in HeLa cells transiently expressing ERK-NLS biosensor along with the V2 vasopressin receptor. Values are means of ΔBRET measured in triplicate ± sd. (D) Dose-response curves for arginine vasopressin (AVP) stimulation. HeLa cells transiently expressing both the sensor and the V2 receptor were stimulated with increasing concentrations of AVP for 10 min followed by BRET2 measurements. Data are mean of ΔBRET ± SEM, n = 3.

cell line. AC16 cells were created via fusion of primary human adult ventricular cardiomyocytes and SV40 transformed and uridine auxotroph human fibroblasts (Davidson et al., 2005). This proliferating human cell line retains the nuclear and mitochondrial DNA of the primary cardiomyocytes as well as other specific cardiomyocyte markers (Davidson et al., 2005). Thus AC16 cells are potentially a useful model to study native cardiomyocyte signaling pathways.

We focused on endogenous angiotensin and muscarinic receptors. qPCR screening demonstrated mRNA expression of AT1R (but not AT2R), M1R, and M3R (data not shown). We assessed activation of the ERK1/2 pathway with angiotensin II, an agonist

for AT1R, and carbachol, an agonist of muscarinic receptors, as well as PMA and EGF, for GPCR-independent pathway activation.

As these cells are difficult to transfect, we used reverse transfection with PEI (see methods Section 2.1) to increase expression of the biosensor. With this protocol, we achieved approximately 15−20% transfection efficacy (data not shown). To increase BRET signal detection, we also used a more sensitive plate reader, the Victor X-Light.

3.4.2 Experimental workflow

1. AC16 cells were seeded overnight over transfection reagent on a white flat-bottom 96-well plate precoated with 0.1% gelatin (see Methods Section 2.1).
2. The medium was removed the next morning to remove nonadherent and dead cells. Fresh complete AC16 medium (see Section 2.1) was then added and the cells were maintained at 37 °C in a 5% CO_2 atmosphere for 36 additional hours.
3. 48 h posttransfection, cells were washed twice with 100 µL of Tyrode's solution at 37 °C and maintained in the plates with 50 µL of the same Tyrode's buffer at 37 °C in a 5% CO_2 atmosphere for an additional 3 h. This additional incubation period following the washes aimed at reducing basal ERK1/2 activation.
4. After 3 h, 50 µL Tyrode's solution at 37 °C containing 10 µM coelenterazine 400a and different concentration of ligands for dose−response curve generation was then added to the wells simultaneously.
5. BRET was assessed as described in Section 2.2 using the Victor X-Light plate reader. Luminescence was measured at 410/80 and 515/30 nm, respectively. Luminescence was recorded every 5 min for the whole plate to obtain kinetics and concentration-response curves. Vehicle was added to other wells and BRET recorded the same way and subtracted from agonist-induced BRET to calculate ligand-promoted BRET expressed as ΔBRET (see Section 2.1).

3.4.3 Results

We first evaluated the capacity to detect ERK1/2 activation with our biosensor in AC16 cells by generating concentration-response curves for PMA (100 fM to 1 µM) and EGF (100 fM to 1 µM) every 5 min for 30 min (Figure 6(A) and (B) show concentration-dependent responses at 10 min). As described in Section 2.2, we used the concentrations yielding the maximal responses for each compound to determine the kinetics of ERK1/2 activation. As we noted in heterologous cell lines, both PMA and EGF promoted a BRET increase reflecting nuclear ERK1/2 activation in AC16 cells ($p < 0.01$) that reached a maximum at 10 min (Figure 7(A)). The data revealed that PMA was more potent and efficacious (Figure 6(A), (B) and (E)) and promoted faster activation of nuclear ERK1/2 than EGF (Figure 7(A)).

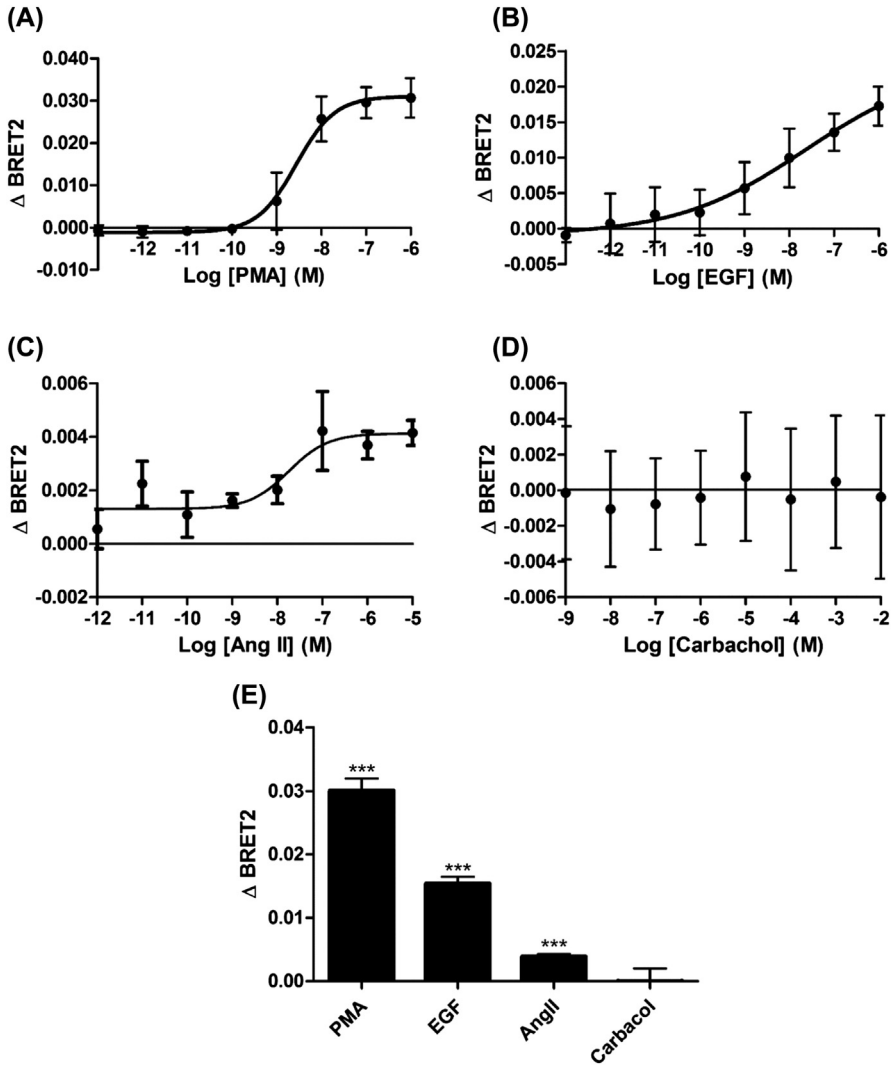

FIGURE 6 Dose-response curve of nuclear ERK1/2 activation in AC16 cells.

Each data point represents ΔBRET induced by 10 min incubation with drugs at different concentrations. (A) Dose-response curve for PMA treatment (n = 5). (B) Dose-response curve following EGF treatment (n = 6). (C) Dose-response curve following Ang II treatment (n = 5). (D) Dose-response curve following carbachol treatment (n = 4). (E) Emax for different drugs at 10 min incubation time. Data represent mean ± SEM (* = $p < 0.05$; ** = $p < 0.01$).

A second series of concentration-response curves was generated to assess nuclear ERK1/2 activity induced by the two endogenous GPCRs present in AC16 cells, AT1, and M1/M3 receptors. We used the same strategy as for GPCR-independent activation to produce concentration-dependant response curves every 5 min and plot kinetics at the Emax ΔBRET values. Figure 6(C) shows dose-response curves at 10 min. The AT1R agonist angiotensin II (1 pM−10 μM) produced a rapid but weak activation of nuclear MAP kinase compared to PMA, reaching a maximum after 5 min of stimulation (Figure 7(B)). In all cases, PMA, EGF, or Ang II, the responses were stable up to 30 min. However, the change in BRET ratio for Ang II was small compared to PMA or EGF. This small change in BRET ratio may make it more difficult to detect nuclear ERK1/2 activation in an endogenous context, so a higher number of replicates should be planned to reduce the variability between experiments. We also stimulated endogenous muscarinic receptors with carbachol (1nM−10 mM). As we saw in heterologous systems, no change in activity for nuclear ERK1/2 was detected following activation of endogenous muscarinic receptor (Figures 6(B), (E) and 7(B)).

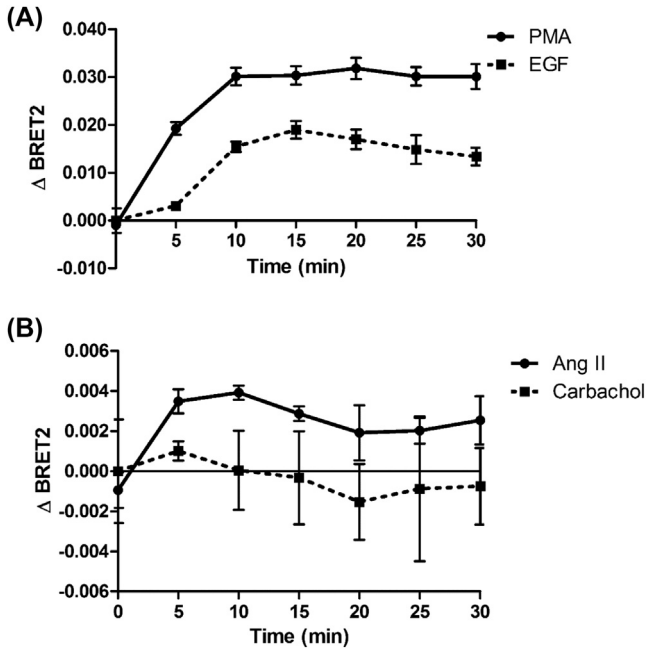

FIGURE 7 Kinetics of nuclear MAP kinase activation in AC16 cells.

Each data point represents the ΔBRET Emax for each dose-response curve at different time points. (A) G protein-coupled receptor-independent activation of nuclear ERK1/2 by PMA (n = 5) and EGF (n = 6). (B) Nuclear ERK1/2 by activation by endogenous receptor ligands angiotensin II (n = 5) and carbachol (n = 4). Data represent mean ± SEM.

4. DISCUSSION

Here, we show that the ability to detect nuclear ERK1/2 using a BRET-based biosensor can vary between cell types and experimental conditions. The sensor readily detected ERK1/2 nuclear activation promoted by strong activators such as PMA and EGF in the three cell types studied with a pharmacology that matched that known for ERK1/2 activation. However, detection of GPCR-promoted activation was highly dependent on receptor expression level and cell type considered. For instance, muscarinic M3 receptor activation could be observed in HeLa cells heterologously expressing the receptor but not when stimulating endogenous receptor expressed at low levels. Such activation could not be observed in HEK 293 cells even following overexpression of the receptor indicating a differential responsiveness between the two cell types that may reflect distinct cellular machineries or differential sensitivities of the biosensor to receptor levels in those cells. Muscarinic M3 receptors seem to activate nuclear ERK1/2 more strongly in HeLa cells than in HEK 293 cells, although would have to be confirmed under conditions where we control the stoichiometry of receptor and biosensor expression more carefully. In contrast to endogenous M1/M3 receptors, endogenous AT1 receptors were able to activate nuclear ERK1/2 signaling in AC16 cells. This is consistent with the known ability of AT1R to stimulate both nuclear and cytosolic ERK1/2 signaling dependent on Gq and β-arrestin, respectively (Tohgo et al., 2002; Wei et al., 2003). This may either indicate that AT1R is better coupled to this pathway than M1/M3 or that AC16 cells express a higher number of AT1R than M1/M3 receptors. In conclusion, we describe the design and use of a BRET-based ERK1/2 sensor engineered to be localized to the nucleus. This biosensor allows us to study ERK1/2 activation in specific cell contexts and can be used to study the mechanisms leading to this activation. This first generation of BRET-based nuclear ERK sensor opens the way for design of similar sensors without an NLS or with an NES that could capture cytosolic responses. These sensors could therefore be multiplexed with the present sensor to assess the relative activation of ERK1/2 in the two compartments. More sensitive biosensors will also be needed to determine if the lack of detection of nuclear ERK1/2 activation in some cell contexts reflects a true difference in the cellular responses or a lack of sensitivity of the sensor used. Although robust and faithful response can be collected with these biosensors, initial characterization and use of such biosensors should involve determining responses to different ligands, different levels of receptor, and different cell types.

ACKNOWLEDGMENTS

This work was supported by a grant from the Consortium Québécois sur la Découverte du Médicament (CQDM) to MB and TH and by grants from the Canadian Institutes of Health Research (CIHR, MOP-130309, TEH; MOP-10501, MB). MB holds a Canada Research Chair

in Signal Transduction and Molecular Pharmacology. NA was supported by a fellowship from the McGill CIHR Drug Development Training Program.

REFERENCES

Busino, L., Chiesa, M., Draetta, G. F., & Donzeli, M. (2004). Cdc25A phosphatase: combinatorial phosphorylation, ubiquitylation and proteolysis. *Oncogene, 23*, 2050−2056.

Chang, L., & Karin, M. (2001). Mammalian MAP kinase signalling cascades. *Nature, 410*, 37−40.

Davidson, M. M., Nesti, C., Panlenzuela, L., Walker, W. F., Hernandez, E., Protas, L., et al. (2005). Novel cell lines derived from adult human ventricular cardiomyocytes. *Journal of Molecular and Cellular Cardiology, 39*, 133−147.

Deng, H., Sun, H., & Fang, Y. (2013). Label-free cell phenotypic assessment of the biased agonism and efficacy of agonists at the endogenous muscarinic M3 receptors. *Journal of Pharmacological and Toxicological Methods, 68*, 323−333.

Dimitri, C. A., Dowdle, W., MacKeigan, J. P., Blenis, J., & Murphy, L. O. (2005). Spatially separate docking sites on ERK2 regulate distinct signaling events in vivo. *Current Biology, 15*, 1319−1324.

Domazet, I., Holleran, B. J., Richard, A., Vandenberghe, C., Lavigne, P., Escher, E., et al. (2015). Characterization of angiotensin II molecular determinants involved in AT1 receptor functional selectivity. *Molecular Pharmacology, 87*, 982−995.

Galés, C., Rebois, R. V., Hogue, M., Trieu, P., Breit, A., Hébert, T. E., et al. (2005). Real-time monitoring of receptor and G-protein interactions in living cells. *Nature Methods, 2*, 177−184.

Harvey, C. D., Ehrhardt, A. G., Cellurale, C., Zhong, H., Yasuda, R., Davis, R. J., et al. (2008). A genetically encoded fluorescent sensor of ERK activity. *Proceedings of the National Academy of Sciences of the United States of America, 105*, 19264−19269.

Kenakin, T., & Christopoulos, A. (2013a). Measurements of ligand bias and functional affinity. *Nature Reviews Drug Discovery, 12*, 483.

Kenakin, T., & Christopoulos, A. (2013b). Signalling bias in new drug discovery: detection, quantification and therapeutic impact. *Nature Reviews Drug Discovery, 12*, 205−216.

Khan, S. M., Min, A., Gora, S., Campden, R., Robitaile, M., Houranieh, G. M., et al. (2015). $G\beta_4\gamma_1$ as a modulator of M3 muscarinic receptor signalling and a novel roles of $G\beta_1$ subunits in the modulation of cellular signalling. *Cellular Signalling, 27*, 1597−1608.

Kim, E. K., & Choi, E. J. (2010). Pathological roles of MAPK signaling pathways in human diseases. *Biochimica et Biophysica Acta, 1802*, 396−405.

Leduc, M., Breton, B., Galés, C., Le Gouill, C., Bouvier, M., Chemtob, S., et al. (2009). Functional selectivity of natural and synthetic prostaglandin EP4 receptor ligands. *Journal of Pharmacology and Experimental Therapeutics, 331*, 297−307.

Luttrell, L. M. (2014). Minireview: more than just a hammer: ligand "bias" and pharmaceutical discovery. *Molecular Endocrinology, 28*, 281−294.

Namkung, Y., Radresa, O., Armando, S., Devost, D., Beautrait, A., Le Gouill, C., et al. (2015). Quantifying biased signaling in GPCRs using BRET-based biosensors. *Methods*. in press.

Sauliere, A., Bellot, M., Paris, H., Denis, C., Finana, F., et al. (2012). Deciphering biased-agonism complexity reveals a new active AT(1) receptor entity. *Nature Chemical Biology, 8*, 622−630.

Sudol, M., & Hunter, T. (2000). New wrinkles for an old domain. *Cell, 103*, 1001−1004.

Thomas, G. M., & Huganir, R. L. (2004). MAPK cascade signalling and synaptic plasticity. *Nature Reviews Neuroscience, 5*, 173−183.

Tohgo, A., Pierce, K. L., Choy, E. W., Lefkowitz, R. J., & Luttrell, L. M. (2002). β-arrestin scaffolding of the ERK cascade enhances cytosolic ERK activity but inhibits ERK-mediated transcription following angiotensin AT1a receptor stimulation. *Journal of Biological Chemistry, 277*, 9429−9436.

Wei, H., Ahn, S., Shenoy, S. K., Karnik, S. S., Hunyady, L., & Luttrell, L. M. (2003). Independent β-arrestin 2 and G protein-mediated pathways for angiotensin II activation of extracellular signal-regulated kinases 1 and 2. *Proceedings of the National Academy of Sciences of the United States of America, 100*, 10782.